Erratum: "Influence of boron doping and hydrogen passivation on recombination of photoexcited charge carriers in silicon nanocrystal/SiC multilayers" [J. Appl. Phys. 114, 073101 (2...

ARTICLE *in* JOURNAL OF APPLIED PHYSICS · AUGUST 2013

Impact Factor: 2.18 · DOI: 10.1063/1.4818332

Influence of boron doping and hydrogen passivation on recombination of photoexcited charge carriers in silicon nanocrystal/SiC multilayers

M. Kořínek, M. Schnabel, M. Canino, M. Kozák, F. Trojánek et al.

Citation: J. Appl. Phys. **114**, 073101 (2013); doi: 10.1063/1.4818332
View online: http://dx.doi.org/10.1063/1.4818332
View Table of Contents: http://jap.aip.org/resource/1/JAPIAU/v114/i7
Published by the AIP Publishing LLC.

Influence of boron doping and hydrogen passivation on recombination of photoexcited charge carriers in silicon nanocrystal/SiC multilayers

M. Kořínek,[1,a)] M. Schnabel,[2] M. Canino,[3] M. Kozák,[1] F. Trojánek,[1] J. Salava,[1] P. Löper,[2] S. Janz,[2] C. Summonte,[3] and P. Malý[1]
[1]*Department of Chemical Physics and Optics, Faculty of Mathematics and Physics, Charles University in Prague, Ke Karlovu 3, 121 16 Prague, Czech Republic*
[2]*Fraunhofer Institute for Solar Energy Systems ISE, Heidenhofstr. 2, 79110 Freiburg, Germany*
[3]*Institute for Microelectronics and Microsystems, Consiglio Nazionale delle Ricerche, via Piero Gobetti 101, I-40129 Bologna, Italy*

(Received 14 June 2013; accepted 29 July 2013; published online 15 August 2013)

The influence of boron (B)-doping and remote plasma hydrogen passivation on the photoexcited charge carrier recombination in silicon nanocrystal/SiC multilayers was investigated in detail. The samples were prepared by high temperature annealing of amorphous (intrinsic and B-doped) $Si_{1-x}C_x$/SiC superlattices. The photoluminescence (PL) intensity of samples with B-doped silicon rich carbide layers was found to be up to two orders of magnitude larger and spectrally red shifted in comparison with that of the other samples. Hydrogen passivation leads to an additional increase in PL intensities. The PL decay can be described well by a mono-exponential function with a characteristic decay time of a few microseconds. This behavior agrees well with the picture of localized PL centers (surface states) together with the passivation of non-radiative defects by boron. The samples with B-doped SiC layers exhibit an additional PL band in the green spectral region that is quenched by hydrogen passivation. Its origin is attributed to defects due to suppression of crystallization of amorphous SiC layers as a result of B-doping. Measurement of ultrafast transient transmission allowed us to study the initial (picosecond) carrier dynamics. It was found to be dependent of pump intensity and interpreted in terms of multiparticle electron-hole recombination. © *2013 AIP Publishing LLC*. [http://dx.doi.org/10.1063/1.4818332]

I. INTRODUCTION

Silicon nanocrystals (Si-NCs) have been known to possess interesting properties such as band-gap modulation with NC size and high sensitivity to surface passivation due to which they are suitable for applications in various fields of science and engineering. Si-NCs are one of the most promising materials for solar cells (non-toxic absorber material in third generation photovoltaics[1,2]), silicon-compatible light sources,[3] biosensors,[4] and nonvolatile memories.[5] Si-NCs embedded in a dielectric matrix provide a material class which is non-toxic and compatible with current Si technology. One of the most promising host materials is SiC due to its appropriate transport properties[6] and ease of doping.[7] The Si-NCs embedded in a SiC matrix can be fabricated by high temperature annealing of amorphous $Si_{1-x}C_x$/SiC superlattices. The use of the so called superlattice approach is expected to give excellent control of NC size, which is limited by the thickness of the silicon rich layer.[8] Moreover, the p-n or p-i-n structure required for carrier separation in a solar cell can be produced by doping the Si-NC superlattice precursor *in-situ*, or by deposition of doped layers of the dielectric material immediately before or after the Si-NCs precursor multilayer in one deposition step.

The transport and recombination properties of Si-NC materials depend on the incorporation of impurities in the host matrix, in the Si-NCs or at the Si-NC interface. As the host matrix consists of SiC NCs as well as amorphous SiC phases after annealing, it is likely to exhibit a high defect density. A passivation of recombination-active defects is therefore required in order to prepare an electronically high-quality material. In this respect, passivation by hydrogen can be used to reduce the concentration of defects in Si-NCs.[9,10] The effect of H incorporation on the PL properties of the B-doped Si-NC/SiC multi-structures has not been investigated yet.

In this paper, we report on the influence of B-doping and hydrogen passivation on the recombination of photoexcited charge carriers in Si-NC/SiC multilayers. In particular, we present results of measurements of (i) a continuous-wave excited photoluminescence as a function of boron doping and remote plasma hydrogen passivation and (ii) time-resolved photoluminescence and transmission under femtosecond pulse excitation.

II. SAMPLES AND EXPERIMENTAL

A. Samples

The samples were prepared using plasma-enhanced chemical vapor deposition (PECVD). Originally 30 amorphous—intrinsic and B-doped—silicon rich carbide (SRC)/stoichiometric SiC bilayers were deposited on quartz glass substrates. The thicknesses of the initial SRC and SiC layers were 3 nm and 6 nm, respectively. The nominal Si atomic fraction in the SRC was 0.65. After deposition, the samples were annealed in fluent N_2:O_2 = 10:1 atmosphere at

[a)]Electronic mail: Miroslav.Korinek@mff.cuni.cz

600 °C for 4 h and then at 1100 °C for 30 min. The samples had a silicon sacrificial layer during annealing to prevent oxidation of the bilayers. During annealing, the sacrificial layer oxidizes and is successively removed by wet etching. Details on the procedure are given in Ref. 11. The high temperature annealing of amorphous $Si_{1-x}C_x$/SiC multilayers resulted in the crystallization of both Si and SiC.[12,13] The polytype of the annealed SiC material is cubic (3 C), with a band gap of ~2.3 eV.[14] Three types of the B-doped samples were studied, in which boron was introduced either within the SRC (SRC-B), within the SiC (SiC-B), or in both layers (Both-B). The intrinsic samples were labeled I. HRTEM analyses carried out on intrinsic $Si_{1-x}C_x$/SiC multilayers processed in the same conditions showed the presence of Si-NCs with a relatively broad size distribution centered around a mean NC diameter of ~3 nm, dispersed all over the film thickness, regardless of the as-deposited multilayer structure. The total c-Si volume in the multilayers after annealing is (8 ± 1) % for all samples. A detailed description of sample preparation is given in Ref. 14. In addition, all samples were broken into two halves and one half underwent remote plasma hydrogen passivation at 450 °C for 45 min. Gas flows were 155 sccm H_2, 50 sccm Ar, 3 sccm O_2.

B. Experimental

In the case of standard continuous-wave excited PL spectroscopy, we used the 442 nm line of a HeCd laser as an excitation source. The PL signal was detected using a CCD camera (Andor iDus) with a spectrometer (Oriel). Excitation power density was ≈3 W/cm^2 (corresponding to a photoexcited carrier density ≈10^{18} cm^{-3}). All spectra were corrected for the spectral sensitivity of the detection system and measured at room temperature. To avoid an interference fringe effect, the PL signal was detected under the Brewster angle.

A femtosecond Ti:sapphire laser system (Tsunami & Spitfire, Newport/Spectra Physics) served as an excitation source for time resolved PL and transient transmission measurements. Parameters of the femtosecond pulses were: repetition rate ~1 kHz, pulse duration ~100 fs, fundamental wavelength 800 nm. The pump pulse with wavelength 400 nm (the second harmonic of the laser output) had an energy fluence from 0.1 to 14 mJ/cm^2, corresponding, on average, to 0.5 to 77 excited electron-hole pairs per NC. The time evolution of PL was investigated using a streak camera (Hamamatsu C5680, single sweep regime, time resolution ≈70 ps) coupled to a spectrograph. The measurement of dynamics of the transient transmission was carried out using a standard pump and probe technique in which the probe pulse monitors the transmission T_E (T_0) of the sample after (without) the pump.[15] We used the second and fundamental harmonic of the laser output as the pump and probe pulse, respectively. Both beams were focused on the sample and spatially overlapped with each other. The spot size of the pump was adjusted to be three times larger than that of probe pulses. The results of time-resolved transmission are presented in the form of normalized transient transmission $\Delta T/T_0 = (T_E - T_0)/T_0$.

III. RESULTS AND DISCUSSION

A. Continuous wave excited PL

The PL spectra of the as-prepared samples are shown in Fig. 1, on the same scale to allow for a direct comparison. The PL spectra of both H-passivated and unpassivated samples are given in Fig. 2. The absorption of all samples at the excitation wavelength was comparable. It is evident that the PL intensity of the samples with B-doped SRC layers is up to two orders of magnitude larger and spectrally red shifted in comparison with that of the other samples.

Apart from the red PL, the sample SiC-B with B-doped SiC barrier also exhibits a PL band centered between 500 and 600 nm, which is either much less significant or not present in the other samples. This band is quenched upon hydrogen passivation (see Fig. 2(c)). It was reported previously[16] that the p-type doping with boron inhibits the crystallization of amorphous SiC films prepared by PECVD technique. Presence of boron can therefore lead indirectly to creation of

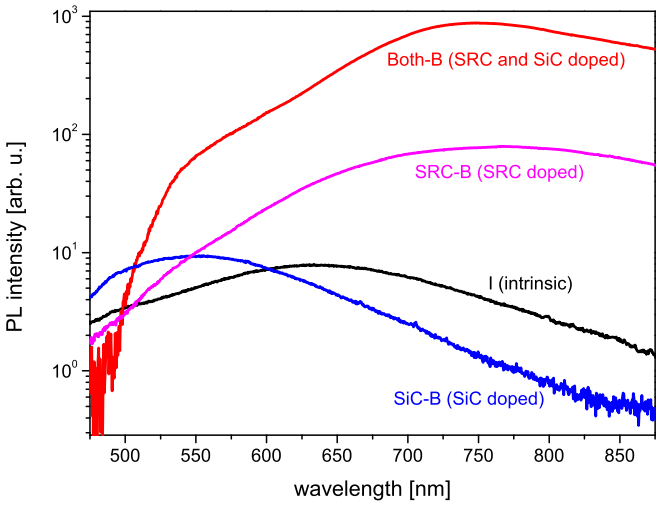

FIG. 1. PL spectra of the as-prepared samples under cw 442 nm excitation.

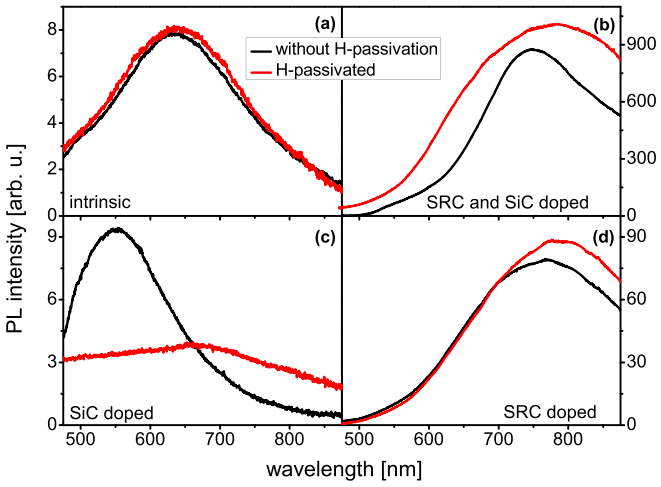

FIG. 2. PL spectra of the samples (a) I, (b) Both-B, (c) SiC-B, and (d) SRC-B under cw 442 nm excitation. Note that the y-axes are different as PL intensities differ by orders of magnitude.

more defects, even though these are not boron-related defects, as it facilitates dehydrogenated amorphous phases.

From Fig. 2, it is clear that the intrinsic samples and H-passivated sample SiC-B have the main PL band centered around 650 nm (Figs. 2(a) and 2(c)). For unpassivated sample SiC-B, this PL band is probably obscured by the band centered in the green spectral region. Doping the SRC layers with boron causes the shift of the PL maximum towards longer wavelengths ≈750 nm (Figs. 2(b) and 2(d)).

Fig. 2 reveals that the effect of the hydrogen passivation depends on whether the SiC or the SRC layer is doped with boron. If the SRC layer (or the SRC and the SiC layers) is doped with boron, hydrogen passivation results into an increase and red shift of PL. If however only the SiC is doped with boron, the H passivation quenches the PL.

Recently, the PL band centered at 1.8 eV (690 nm) was observed for intrinsic samples prepared in a similar way.[17] This PL signal was found to be strongly reduced after hydrogen passivation and it is most likely due to the radiative recombination of carriers at defect states correlated with SiC NCs. In our measurements, the effect of H-passivation on the PL of the intrinsic sample does not exceed the experimental error.

The obtained characteristics of the samples with B-doped SRC layers may be affected by boron incorporation at the surface of Si-NCs.[18–20] Recent theoretical studies[18,20] show that boron prefers residing at the surface of Si-NCs introducing significant energy levels within the energy band gap. The incorporated boron can also passivate non-radiative defects at the Si-NCs/SiC interface, and therefore, causes increase in PL intensity. The PL intensity increase due to doping was reported previously in phosphorus-doped Si-NCs.[21,22] The difference in PL intensities of the samples, Both-B and SRC-B may be due to an additional presence of the optical transition from the conduction band to the B-level in bulk SiC in sample Both-B. Despite the fact that the sample SiC-B also has B-doped SiC layers, this transition may not occur because of the aforementioned suppression of amorphous SiC crystallization by boron. To confirm the presence of a large concentration of defects in the sample SiC-B, we performed X-ray diffraction and conductivity measurements (results of these measurements are not presented in this paper). The observed significant amount of amorphous SiC and very low conductivity confirmed this assumption.

The band at ≈550 nm present in the B-doped SiC sample is quenched by hydrogen passivation, so this band can clearly be attributed to recombination via defects, most likely dangling bonds. That the hydrogen passivation succeeded in quenching this PL band also shows that it succeeds in diffusing into the multilayers (which has not been known a priori, see Ref. 23). As we have no reason to suspect that hydrogen diffusion into the sample SiC-B is better than into the other samples, and as the PL of samples Both-B and SRC-B is not quenched, but slightly increased by hydrogen passivation, the latter is definitely not related to dangling bonds, but enhanced by passivation of dangling bonds.

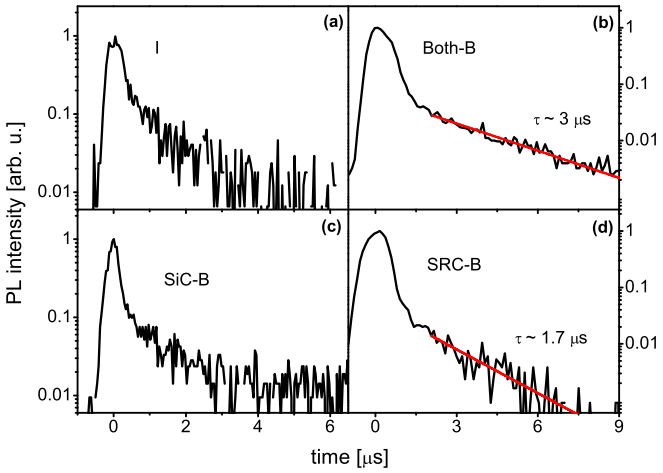

FIG. 3. Normalized microsecond PL dynamics recorded at spectral maxima of the samples (a) I, (b) Both-B, (c) SiC-B, and (d) SRC-B.

B. Time-resolved measurements

The microsecond PL dynamics recorded in the 60 nm spectral interval near the maximum of the time-integrated PL spectra are shown in Fig. 3. The PL signals of the I and SiC-B samples are much weaker than those of the samples with B-doped SRC, so it is not possible to perform a detailed analysis of the time evolution of PL for these samples. The microsecond tail of the PL decay of the samples with B-doped SRC can be described well by a mono-exponential decay function (see Figs. 3(b) and 3(d)). Mono-exponential decay is generally typical of localized PL centers.[24] Lifetimes of 3 and 1.7 μs were obtained for samples Both-B and SRC-B, respectively. These characteristic decay times were found to be excitation intensity independent.

The measurement on a shorter time scale reveals that the PL dynamics contain—apart of the microsecond decay—also a picosecond component, see Fig. 4(a). As the time resolution of PL measurements is limited to approximately 70 ps, we also used time-resolved transmission with a time resolution of 200 fs to obtain more detailed data on the initial

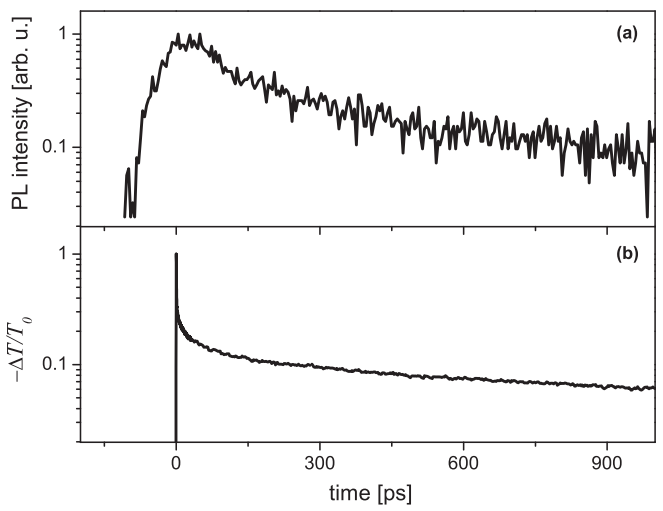

FIG. 4. (a) Normalized picosecond PL dynamics at 730 nm, sample Both-B, laser fluence 14 mJ/cm^2. (b) Normalized dynamics of transient transmission at 800 nm, sample Both-B, laser fluence 10 mJ/cm^2.

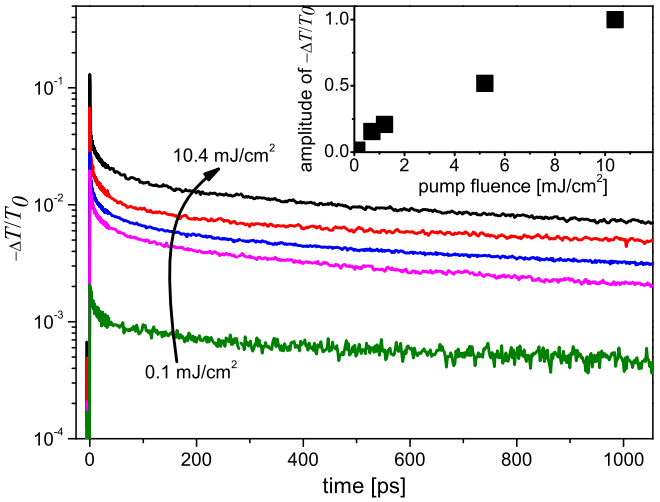

FIG. 5. Dynamics of transient transmission of the sample Both-B, excited by various excitation pump fluencies (0.1, 0.5, 1.0, 5.2, and 10.4 mJ/cm^2). Inset—the dependence of initial amplitude of transient transmission on pump fluence.

carrier dynamics. In time-resolved transmission, the photon energy of the probe beam is tuned below the absorption edge of the NCs such that only the absorption due to photoexcited carriers is monitored; which leads to a negative signal of transient transmission. The time evolution of differential transmission follows the dynamics of photoexcited carrier density. In Fig. 4, we compare the time-resolved PL with the time-resolved transmission measurements. We can clearly see that both dynamics have similar time evolution on the longer time scale. However, they seem to differ significantly in the initial part of the decay which is probably due to the different time resolution of both measurements (compare also the resolution-limited rise edges of both dynamics in Fig. 4).

In Figure 5, we display the dynamics of transient transmission at 800 nm for different pump fluences. The number of initially photoexcited carriers scales linearly with the excitation fluence as can be seen from a linear scaling of the

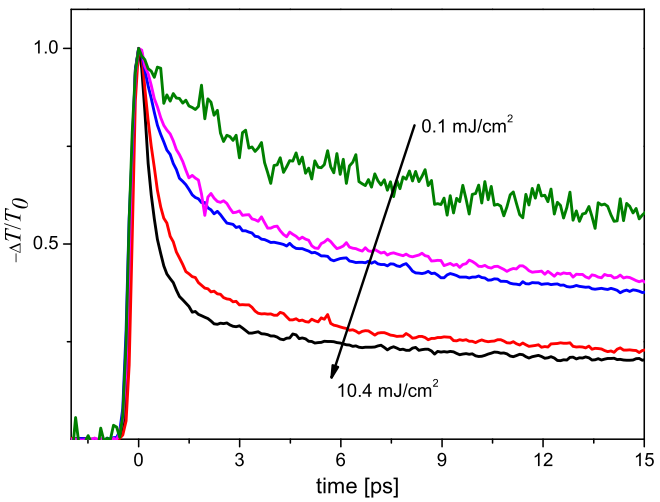

FIG. 6. Normalized dynamics of transient transmission of the sample Both-B, excited by various excitation pump fluencies (0.1, 0.5, 1.0, 5.2, and 10.4 mJ/cm^2).

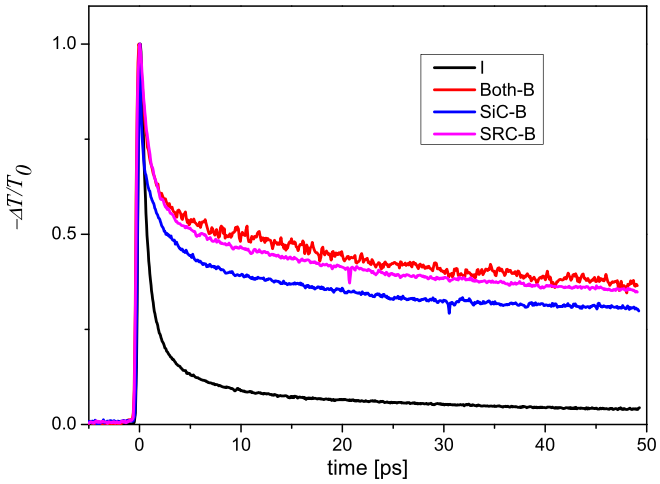

FIG. 7. Normalized dynamics of transient transmission of the samples, pump fluence 1.3 mJ/cm^2. The time evolution of differential transmission reflects the dynamics of the photoexcited carrier population.

peak transient transmission (see the inset of Fig. 5). However, the initial (<10 ps) part of the dynamics is intensity dependent being more pronounced for higher pump fluences, see Fig. 6. This nonlinear fast picosecond dynamics is most likely related to multi-particle non-radiative recombination (Auger[25,26] or bimolecular[27] processes).

The dynamics of transient transmission at 800 nm for the samples are shown in Figure 7. Note that the absorption of all samples is approximately the same resulting in a photoexcited charge carrier density of ~6–7 electron-hole pairs per NC (calculated by using known absorption and laser fluence and assumed average NC size ≈3 nm). It is evident that the transient transmission decays of all the B-doped samples are much slower than that in the intrinsic sample. In addition, the samples with B-doped SRC layers have almost identical dynamics. This can be interpreted in terms of creation of new energy states into which photoexcited carriers can be effectively transferred before they are able to recombine via multiparticle recombination.

IV. CONCLUSION

P-type doping with boron and remote plasma hydrogen passivation have a dramatic effect on the recombination of photoexcited charge carriers in Si-NC/SiC multilayers. Our results suggest that hydrogen passivation can deactivate the defect centers which are responsible for non-radiative recombination.

PL measurements show that the PL signal of the samples with B-doped SRC layers is up to two orders of magnitude larger than that of the other samples and their PL maximum is shifted towards longer wavelengths. The measurements of the PL decay on a microsecond time scale reveals a mono-exponential decay typical of recombination of carriers trapped in localized centers. We attribute the increase in PL intensity to the passivation of non-radiative defects at the Si-NCs/SiC interface by boron. We interpret the difference in PL intensities between the sample with B-doped SRC layers and that with B-doped SRC/SiC bilayers in terms of the SiC conduction band—B-level transition in the latter sample.

The sample with B-doped SiC layers exhibits a PL band centered in the green spectral region that is quenched by hydrogen passivation. The origin of this PL band is related to defects formed as a consequence of suppression of amorphous SiC crystallization due to B-doping.

The picture of photoexcited charge carrier dynamics is completed by the measurements of differential transmission on a picosecond time scale. The picosecond dynamics is dependent of pump intensity and can be interpreted in terms of multiparticle recombination. The transmission decay rates in all the B-doped samples are much slower than that in the intrinsic sample. This can be understood as a consequence of creation of new energy states into which charged carriers can be transferred before they can undergo multiparticle recombination.

Given that Si-NCs embedded in SiC have always shown relatively good absorption and conduction, with their suitability for optoelectronic devices compromised only by their short minority carrier lifetime, the results presented here are a key step towards the realization of minority carrier devices from Si-NCs in SiC.

ACKNOWLEDGMENTS

We acknowledge the financial support of the EU 7th Framework Program *"Silicon Nanodots for Solar Cell Tandem"* (NASCEnT) under Contract No. 245977 and of the Charles University in Prague (Project Nos. GAUK 443911 and SVV-2013-267306).

[1]G. Conibeer, M. Green, E.-C. Cho, D. König, Y.-H. Cho, T. Fangsuwannarak, G. Scardera, E. Pink, Y. Huang, T. Puzzer, S. Huang, D. Song, C. Flynn, S. Park, X. Hao, and D. Mansfield, Thin Solid Films **516**, 6748 (2008).
[2]M. A. Green, *Third Generation Photovoltaics, Advances Solar Energy Conversion* (Springer, Berlin, 2003), p. 72.
[3]L. Pavesi, J. Phys.: Condens. Matter **15**, R1169 (2003).
[4]A. Jane, R. Dronov, A. Hodges, and N. H. Voelcker, Trends Biotechnol. **27**, 230 (2009).
[5]S. Tiwari, F. Rana, H. Hanafi, A. Hartstein, E. F. Crabbé, and K. Chan, Appl. Phys. Lett. **68**, 1377 (1996).
[6]D. Song, E.-C. Cho, G. Conibeer, Y. Huang, C. Flynn, and M. A. Green, J. Appl. Phys. **103**, 083544 (2008).
[7]G. L. Harris, *Properties of Silicon Carbide* (INSPEC, Institution of Electrical Engineers, London, 1995), p. 153.
[8]M. Zacharias, J. Heitmann, R. Scholz, U. Kahler, M. Schmidt, and J. Bläsing, Appl. Phys. Lett. **80**, 661 (2002).
[9]S. P. Withrow, C. W. White, A. Meldrum, J. D. Budai, D. M. Hembree, Jr., and J. C. Barbour, J. Appl. Phys. **86**, 396 (1999).
[10]S. Cheylan and R. G. Elliman, Appl. Phys. Lett. **78**, 1225 (2001).
[11]M. Canino, C. Summonte, M. Allegrezza, R. Shukla, I. P. Jain, M. Bellettato, A. Desalvo, F. Mancarella, M. Sanmartin, A. Terrasi, P. Löper, M. Schnabel, and S. Janz, Mater. Sci. Eng. B **178**, 623 (2013).
[12]C. Summonte, M. Canino, M. Allegrezza, M. Bellettato, A. Desalvo, S. Mirabella, and A. Terrasi, in *Proceedings of the 26th European PV Solar Energy Conference and Exhibition on Systematic Characterization of Silicon Nanodot Absorption for Third Generation Photovoltaics*, Hamburg, Germany, 5–9 September 2011.
[13]J. López-Vidrier, S. Hernández, J. Samà, M. Canino, M. Allegrezza, M. Bellettato, R. Shukla, M. Schnabel, P. Löper, L. López-Conesa, S. Estradé, F. Peiró, S. Janz, and B. Garrido, Mater. Sci. Eng. B **178**, 639 (2013).
[14]C. Summonte, M. Canino, M. Allegrezza, M. Bellettato, A. Desalvo, R. Shukla, I. P. Jain, I. Crupi, S. Milita, L. Ortolani, L. Lopez-Conesa, S. Estrade, F. Peiro, and B. Garrido, Mater. Sci. Eng. B **178**, 551 (2013).
[15]P. Malý, Czech. J. Phys. **52**, 645 (2002).
[16]M. Schnabel, A. Witzky, P. Löper, R. Gradmann, M. Künle, and S. Janz, in *Proceedings of the 26th European PV Solar Energy Conference and Exhibition on Electrical Properties of Recrystallised SiC Films from PECVD Precursors for Silicon Quantum Dot Solar Cell Applications*, Hamburg, Germany, 5–9 September 2011.
[17]M. Künle, T. Kaltenbach, P. Löper, A. Hartel, and S. Janz, Thin Solid Films **519**, 151 (2010).
[18]X. Pi, X. Chen, and D. Yang, J. Phys. Chem. C **115**, 9838 (2011).
[19]H. Sugimoto, M. Fujii, M. Fukuda, K. Imakita, and S. Hayashi, J. Appl. Phys. **110**, 063528 (2011).
[20]Y. Ma, X. Chen, X. Pi, and D. Yang, J. Nanopart. Res. **14**, 802 (2012).
[21]S. H. M. Fujii, A. Mimura, and K. Yamamoto, Appl. Phys. Lett. **75**, 184 (1999).
[22]A. Mimura, M. Fujii, S. Hayashi, D. Kovalev, and F. Koch, Phys. Rev. B **62**, 12625 (2000).
[23]K. Ding, U. Aeberhard, W. Beyer, O. Astakhov, F. Köhler, U. Breuer, F. Finger, R. Carius, and U. Rau, Phys. Status Solidi A **209**, 1960 (2012).
[24]I. Pelant and J. Valenta, *Luminescence Spectroscopy of Semiconductors* (Oxford University Press, Oxford, 2012), p. 85.
[25]I. Mihalcescu, J. C. Vial, A. Bsiesy, F. Müller, R. Romestain, E. Martin, C. Delerue, M. Lannoo, and G. Allan, Phys. Rev. B **51**, 17605 (1995).
[26]K. Ueda, T. Tayagaki, M. Fukuda, M. Fujii, and Y. Kanemitsu, Phys. Rev. B **86**, 155316 (2012).
[27]P. Malý, F. Trojánek, J. Kudrna, A. Hospodková, S. Banáš, V. Kohlová, J. Valenta, and I. Pelant, Phys. Rev. B **54**, 7929 (1996).